A Moving Solar Roof for a Hybrid Solar Vehicle

G.Coraggio*, C.Pisanti*, G.Rizzo*, A.Senatore*

**Dept. of Mechanical Engineering, University of Salerno, 84084 Fisciano (SA), Italy*

Email: gcoraggio - cpisanti – grizzo – a.senatore @unisa.it

Abstract: A study on the benefits of a moving solar roof for parking phases in a Hybrid Solar Vehicle is presented. A kinematic model of a parallel robot with three degrees of freedom has been developed and validated over the experimental data obtained by a small scale real prototype. The effects of roof design variables are analyzed, and the benefits in terms of net available energy assessed by simulation over hourly solar data at various months and latitudes. The structure of a model based control to achieve the optimal orientation of the solar roof is also presented.

Keywords: Tracking systems, Solar energy, Hybrid vehicles.

1. INTRODUCTION

In last years there is a substantial awareness about sustainable mobility issues, in order to reduce fossil fuel depletion and greenhouse effects related to personal mobility. Besides other solutions, an increasing attention is being paid to the integration of Hybrid Electric Vehicles (HEV) and Photo-Voltaic (PV) sources (Letendre et al, 2003; Rizzo, 2010), as confirmed by the recent launch of a HEV mounting solar panels by a major automotive company. Hybrid Solar Vehicles (HSV) can give substantial benefits to fuel economy and emissions, especially in the case of intermittent use in urban driving (Arsie et al., 2007, 2008 I,II). Moreover, their economic feasibility may be achieved in a near future, also thanks to the decreasing cost (Fig. 1) and to the increasing efficiency of photovoltaic panels .

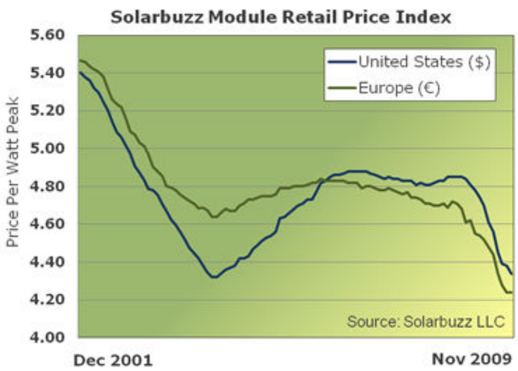

Fig. 1 – Trends in photovoltaic panels price

The additional costs of HSV with respect to HEV are mainly due to photovoltaic panels, that in solar cars are used at fixed, almost horizontal, position. As known, solar irradiance on a tilted surface is the sum of direct, diffuse and reflected components (Quaschning, 2003). The amount of direct solar energy captured by the surface depends on the angle of incidence, defined as the angle between sun rays and the perpendicular to the surface (Fig. 2):

$$E_C = E_i \cdot \cos i \quad (1)$$

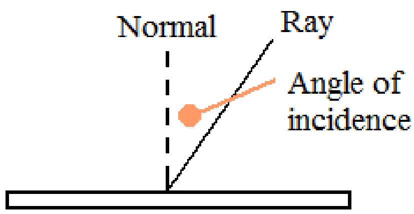

Fig. 2 – Angle of incidence

Although in last years different solutions of moving panels are being adopted in fixed photovoltaic plants, this option has not been considered until now on solar cars, where PV panels are fixed and located in an almost horizontal position. In pure solar cars, that have no or little storage capacity, the instability and the additional weight, complexity and aerodynamic losses related to the use of a moving roof would not compensate the benefits. Moreover, the energy spent to orient the panel during driving can be much greater that the energy required on a fixed plant, if car orientation is often varying.

The picture can be different if moving solar panels are adopted on an electric or a hybrid vehicle, provided with a battery of adequate capacity. Previous studies, as well as simple energy balances, demonstrate that the relative benefits of solar energy are quite significant (up to 30%) when the car is used for one or two hours per day in urban driving, as it happens for a large number of users [Statistics for Road Transport, UK Government]. In this case, a large part of the solar energy is captured during parking time, and the adoption of a tracking system just when the car is parked would not cause the drawbacks before mentioned. On the other hand, there are some specific aspects that make the study of a moving roof on a car, even if only when parked, different from a fixed plant, since: i) car orientation during

parking is not fixed, ii) aerodynamic losses and additional weight should be minimized, iii) perfect orientation, as in an ideal two-axis tracking system (Fig. 3), could not be achieved in all conditions due to kinematic constraints.
In order to evaluate the benefits of a moving solar roof, the effects of roof orientation must be estimated. A solar calculator, based on the analysis of time series of solar radiation in US cities over about 30 years, has been used [www.nrel.gov/rredc/pvwatts] to estimate the relative gain on the yearly average solar energy achievable on a fixed PV plant by the adoption of a 2-axis tracking PV array (Fig. 3) with respect to the horizontal position. The results are presented in Fig. 4, for different latitudes. It emerges that the adoption of moving panels can give a significant improvement in the annual solar energy, particularly at high latitudes.

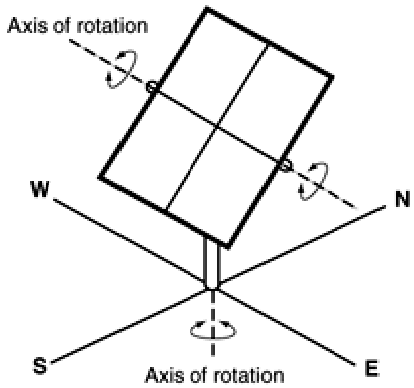

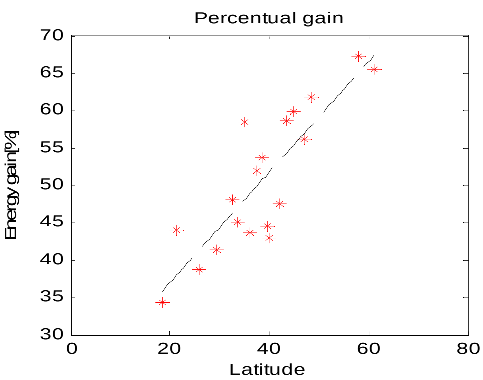

Fig. 4 – Relative gain in yearly solar energy of an ideal two-axis tracking PV array with respect to a fixed one (horizontal)

The relative gain also depends on the month: for example, in Los Angeles the minimum gain (about 21%) is in the summer, while the maximum value, up to 100%, is achieved in winter time. The fraction of reflected energy has also a significant influence on the energy captured: the reflected energy by the soil does not impact on the horizontal panel, while it can be partly captured by an inclined panel.
The abovementioned results are referred to a fixed plant, while in case of a mobile roof on a vehicle additional considerations should be done. In this case, the increase in collected energy is extended only to parking time, while the tracking system should minimize its negative impacts on aerodynamics and weight during driving and, of course, on costs.

In next chapters, a kinematic model of a moving solar roof as a parallel robot with three degrees of freedom is presented, and validated over the experimental data obtained by a small scale real prototype. The effects of roof design variables are analyzed, for different geometries, and the benefits in terms of net available energy are assessed by simulation over hourly solar data at various months and latitudes, also considering the energy spent to move the roof. The structure of a control system to achieve the optimal orientation of the solar roof is also presented.

2. THE PROPOSED SOLAR ROOF

In order to test the feasibility of such proposal, a prototype of mobile solar roof, to be oriented only during parking hours, is being developed at the University of Salerno.
The mobile roof has been designed as a parallel robot: it allows three degrees of freedom, while the orientation of the roof is performed with three displacements generated by three separate motors, connected to a PLC (Programmable Logic Controller). An algorithm in Matlab generates the input for PLC, to realize the desired panels orientation.

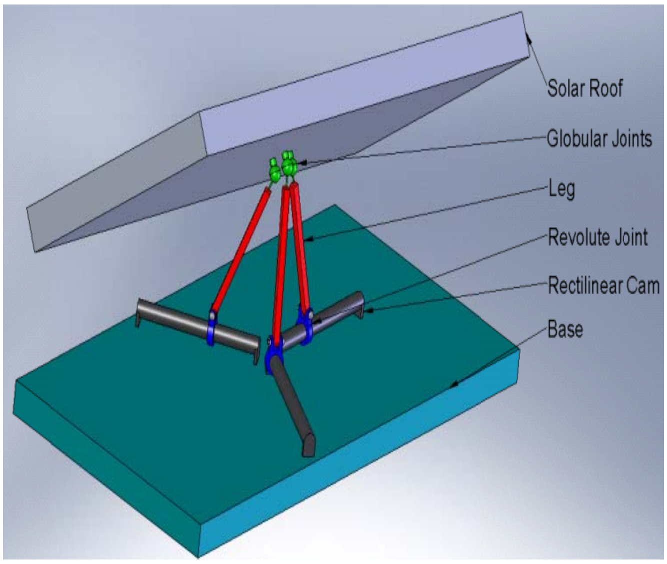

Fig. 5 – The model of moving roof realized with Solid Works

The roof kinematic system is a 3-dof triaglide PKM (Parallel Kinematics Machine) with constant leg length, actuated rectilinear cam joint on the base and a passive globular joint below the mobile roof, which is the tool center point of the PKM (Tsai, 1999). The rectilinear motion is allowed by a guided screw-nut system driven by DC motor. At the rest position, the slidings of rectilinear cams s_i have their minimum value, and the angle between axes of actuations and the legs has the value α_0. Such angle should be enough small to limit the height of the roof at rest, but should also ensure a sufficient lever arm to allow to start moving the roof.
The study of the roof has been performed through a kinematic model implemented in Matlab, described in section 3 and in previous references (Pisanti, 2008). The model has also graphical capabilities (Fig. 6). Moreover, VR (Virtual Reality) CAD simulation has been developed with SolidWorks (Fig. 5) (Coraggio, 2008). Both the models have

been validated over the data measured on a small scale prototype (Fig. 7).

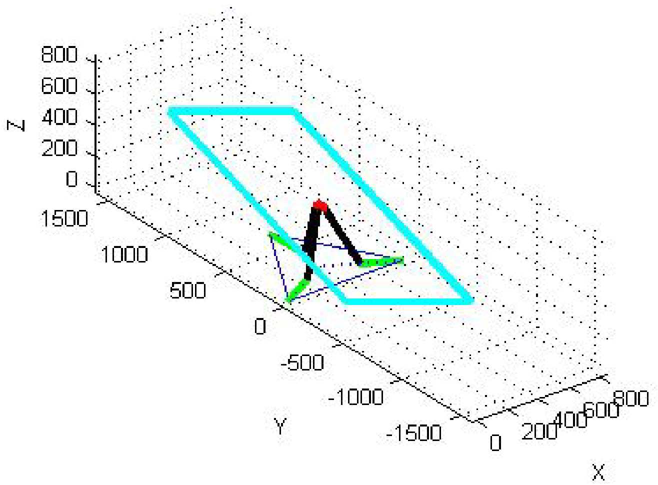

Fig. 6 – Graphical output by the Matlab model

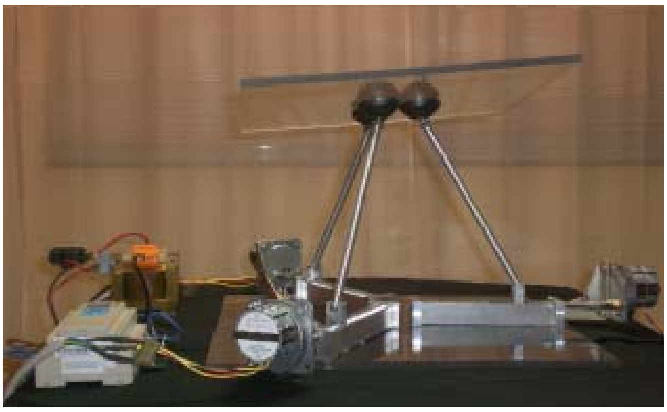

Fig. 7 – Small scale prototype of moving solar roof

3. THE KYNEMATIC MODEL

The roof geometry is evaluated by means of the kinematic model (A.1) - (A.8) by solving a problem of constrained optimization:

$$min_x f(x) \qquad (2)$$

subject to the constraints:

$$G_i(x) \leq 0 \qquad (3)$$

and

$$E_i(x) = 0 \qquad (4)$$

The six decision variables x are represented by the three sliding s_i of rectilinear cam and the three angles α_i between the axes of actuations and their prismatic joint. The objective function f(x) to be minimized is the angle of incidence between the sun ray and the normal to the roof plane (Fig. 2). The equality constraints E(x) express the condition that the computed values of the three legs $l_{ci,j}$ are equal to the assigned value l. The inequality constraints G(x) express the condition of no interference between i) the solar roof and the vehicle (i.e. the quote z should be greater than zero for all the points), and ii) between the legs and the solar roof. When the constraints (3) are satisfied, the roof can be oriented exactly toward the sun, otherwise it would be oriented in the "best" way, to maximize the direct component of solar energy.

To know how to orient the mobile roof is necessary to compute declination δ and solar height ϑ_s, as a function of latitude φ, hour angle h, and year day N:

$$\delta = -23.45 \cdot cos\left(\frac{2\pi(N+10)}{365}\right) \qquad (5)$$

$$h = -180 + 360\,\frac{hour}{24} \qquad (6)$$

$$\vartheta_s = arcsin(cos(h) \cdot cos(\delta) \cdot cos(\varphi) + sin(\delta) \cdot sin(\varphi)) \qquad (7)$$

The direction of the sun ray, defined by angles $\beta_{x,opt}$ e $\beta_{x,opt}$, can be then computed as a function of the relative azimuth $\Phi_s - \Phi_v$ between sun and vehicle:

$$A_1 = \cos(\vartheta_s) \cdot \sin(\Phi_s - \Phi_v) \qquad (8)$$

$$B_1 = \cos(\vartheta_s) \cdot cos(\Phi_s - \Phi_v) \qquad (9)$$

$$C_1 = \sin(\vartheta_s) \qquad (10)$$

$$\beta_{x,opt} = arctg\left(-\frac{A_1}{C_1}\right) \qquad (11)$$

$$\beta_{y,opt} = arctg\left(-\frac{B_1}{C_1}\right) \qquad (12)$$

To orient the roof exactly toward the sun, these two angles must coincide with the angles formed by the normal of the roof.

The problem (2) - (4) is solved by means of classical 2^{nd} order optimization algorithms (Augmented Lagrangian approach combined with Quasi-Newton algorithm), implemented in the optimization tool of Matlab. Computational time is order of few seconds, on a Sony VAIO PC.

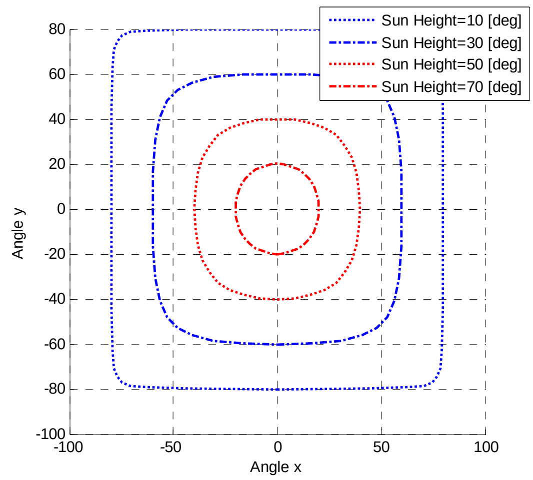

Fig. 8 – Roof angles at different sun height

The position of the roof with respect to the vehicle can be characterized by the angles between the roof plane and the axes β_x and β_y (A.8), oriented toward vehicle width and length respectively (Fig. 6). The angles corresponding to sun position at different sun height and for various orientations of the vehicle (relative azimuth of vehicle respect to sun) can be also computed by (11) and (12). Obviously, the orientation toward lower values of sun height (at daylight or sunset, or at high latitudes) requires to actuate higher values of roof angles (Fig. 8). It can be also observed that at higher sun height the curves are almost circular, and tend to be square at lower values.

4. STUDY AND OPTIMIZATION OF ROOF GEOMETRY

A systematic study has been carried out to observe the effects of the geometric variables on the performance of the roof, in terms of its capability to be oriented toward a large angular range. The study has been performed by determining numerically the limit conditions corresponding to incipient interference (i.e. $G_i(x)=0$) for various angles.
The calculation of this limit angles has been made for different geometry of the mobile roof: for each geometry represented in next figure, it took about 7 minutes, with a PC Intel(R) Core(TM) i7 CPU 920 @2.67GHz, 8183 MB RAM.

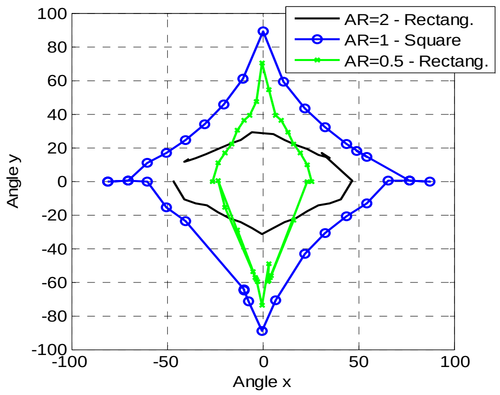

Fig. 9 – Effects of aspect ratio

In terms of aspect ratio AR, defined as the ratio between roof length and width, the best results are obtained when the dimensions of the roof are equal (AR=1), while for a rectangular shape a smaller angular range can be reached (Fig. 9).

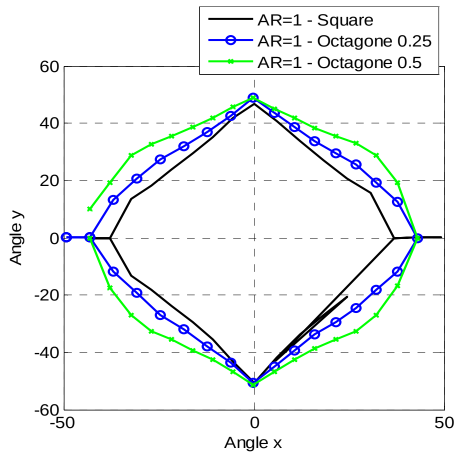

Fig. 10 – Effects of bevelling

The interference with the vehicle occur in correspondence of the roof vertices. The adoption of bevelling can therefore allow reaching a larger angular range (Fig. 10). Of course, bevelling also reduces the net area for solar panels. Therefore, these aspects have to be examined jointly. The effect of the length of legs ***r*** and of the distance between the globular joints ***l*** has been studied. The best results are obtained with the highest values of ***r*** and the smallest values of ***l***, compatibly with space constraints and the stability of the roof (Fig. 11).

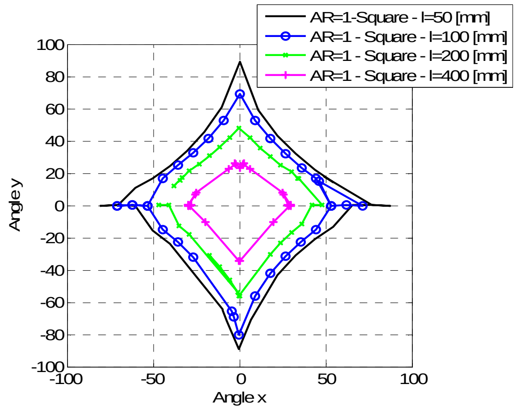

Fig. 11 – Effects of the distance between the globular joints

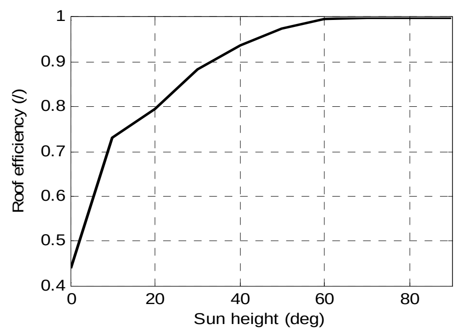

Fig. 12 – Average roof efficiency vs. sun height

In order to characterize each roof in terms of energy efficiency, the mean value of cos(***i***) can been evaluated for different values of solar height. Since optimal vehicle orientation (i.e. azimuth) could not be realized in most practical cases, due to space constraints in the parking places, for each sun height the efficiency is averaged over all azimuth angles, from 0° to 360°. An example corresponding to rectangular roof shape is shown in Fig. 12.

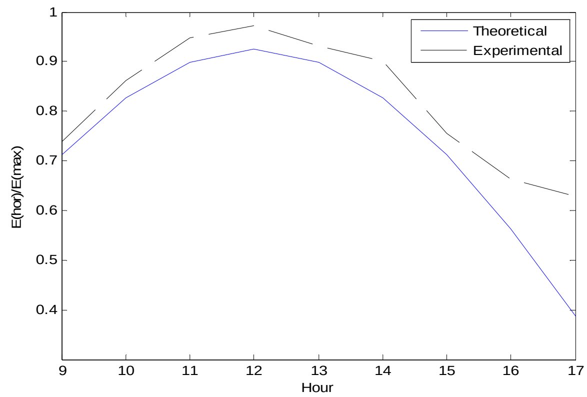

Fig. 13 – Energy fraction at horizontal position. Theoretical vs experimental values (Fisciano, May 2010).

It has to be remarked that the ratio between energy taken at horizontal position and the maximum one is not necessarily equal to the value provided by equation (1), since diffuse and reflected components may be present, and also since kinematic constraints may prevent from reaching optimal orientation. A comparison of theoretical and experimental values, obtained by a pyranometer mounted on the roof prototype (Fig. 7) is presented in Fig. 14. It can be observed that, although the trends are similar, some significant differences can occur, particularly at lower sun height (late afternoon).

5. SIMULATION OVER HOURLY SOLAR DATA

Finally, a detailed analysis of the expected benefits of a moving solar roof has been performed by using hourly solar data available for different US cities [www.nrel.gov/rredc/pvwatts].
The database provide the measured net power for a 2-axis tracking roof and for a fixed roof at horizontal position. For each hour, the sun height is evaluated, and the average roof efficiency with respect to the ideal 2 axis roof computed by the relative efficiency curve (Fig. 12). The comparison of the energy collected on monthly basis in Los Angeles, normalized respect to its maximum value, is presented in Fig. 14, while an analysis on yearly basis for four different locations at various latitudes is shown in Tab. 1. The results demonstrate that the proposed moving solar roof, even taking into account the kinematic constraints that do not allow perfect orientation, allows a significant gain in energy with respect to the horizontal panel, approaching the ideal 2 axis solution. The gain with respect to horizontal position range from 30% at low latitudes up to 47% at highest ones.

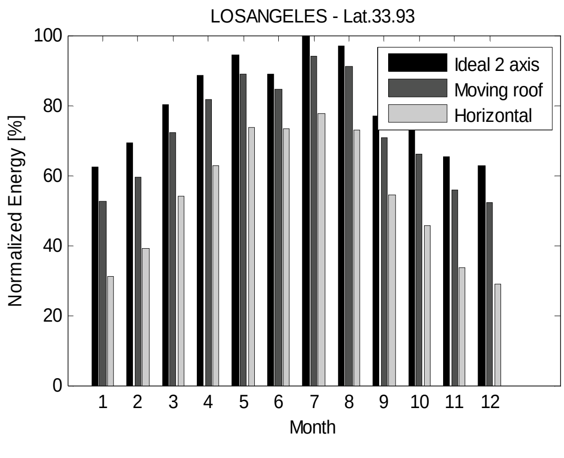

Fig. 14 – Energy collected with various options of solar roof (Los Angeles, 1988)

Location	Latitude	A	B
Honolulu	21.33	46.57	30.70
Los Angeles	33.93	48.48	34.38
Chicago	41.78	52.27	35.83
Anchorage	61.17	78.74	46.89

Tab. 1 – Yearly percent gain with respect to horizontal position for ideal two axis (A) and real mobile roof (B)

It is timely to remark that these results have been obtained with a roof of rectangular shape, without bevelling, which efficiency is shown in Fig. 12. Even better results are expected by adopting an optimized geometry, as discussed in previous paragraphs. A trade-off between the benefits due to better orientation properties and the reduction in solar surface due to bevelling and to the adoption of a non rectangular shape should be also performed. It emerges that the design of the solar roof would be strictly connected to the design of the vehicle itself, impacting on its dimensions and shape, as well as on weight, aerodynamics and, of course, fuel consumption, emissions and cost.

6. MECHANICAL ENERGY REQUIRED TO ACTUATE SOLAR ROOF MOTION

According to the roof kinematics and the involved mechanisms introduced in the Section 3, the contact along the screw/nut surfaces in relative motion may be analyzed by means of forces projection on a sloped plane with respect to the screw axis. Say ω the rotational speed of the screw, M_m the DC motor torque, r_m the screw radius, the following calculation of the mechanical work required for a general s_1-s_2 stroke of the leg base slider may be performed:

$$L_m = \int_{\theta(s1)}^{\theta(s2)} M_m(\theta)d\theta = \int_{\theta 1}^{\theta 2} F(\theta) r_m \tan(\alpha + \varphi)\, d\theta = r_m \tan(\alpha+\varphi) \int_{\theta 1}^{\theta 2} \frac{W_L(roof\_orientation)}{\cos\beta(roof\_orientation)} d\theta \quad (13)$$

Say μ and φ the friction coefficient and the friction angle (μ = tan φ) respectively, by taking into account the design constraints, the need to achieve an irreversible mechanism and boundary lubrication regime between screw and nut, a good assessment of the mechanical efficiency of the transmission, with φ≈α=10° is given by:

$$\eta_m = \frac{\tan\alpha}{\tan(\alpha+\varphi)} \approx 0.48 \quad (14)$$

Assuming a motor speed of 100 rpm and a pitch of 3 mm, corresponding to a stroke of 300 mm in 60 s, a roof weight of 500 N, an axial force F equal about to 200 N, a mechanical work of about 460 J for each slider results by (13) and (14). Considering a roof energy gain equal to 30% and assuming an average power of 200 W for the solar roof in horizontal position, the energy spent to move the roof would be restored in about 23 s.
The evaluation of the mechanical work spent can be also integrated in to the roof model, to estimate the time required to restore the energy spent based on actual conditions. This feature will be used within the model based control depicted in the following paragraph, in order to decide if the roof should be actuated or not (for instance, this occurrence may result for low insulation in the late afternoon, and during night of course).

7. TOWARD A MODEL BASED CONTROL OF SOLAR ROOF

The presented models represent the basis to develop a model based control system for the moving solar roof during parking phases. A possible scheme, including both feed-forward and feedback control, is shown in Fig. 15.
A GPS module provides vehicle position (latitude, longitude) and orientation (azimuth), and also actual date and time. The

sun position (height, azimuth) is computed, and the optimal roof angles (β_x, β_y) that maximize direct solar energy are evaluated. The energy to be spent to move the roof is also estimated. Then, starting from the actual solar power and roof position, the minimum parking time to achieve a positive gain in net energy is estimated. If the minimum parking time is lower than the expected duration of parking phase, the tracking system is actuated. The positions of rectilinear cams corresponding to the given angles (β_x, β_y) are read by a look-up table, previously computed by the presented kinematic model, and their values are actuated by the tracking system (step-by-step motors).

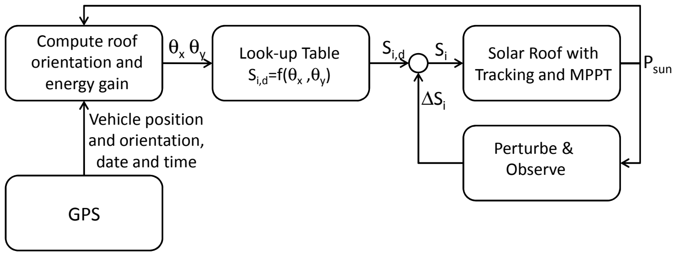

Fig. 15- Structure of solar roof control system

In real cases, it could happen that the position that maximizes the global energy may be different from the computed one, due to the presence of the diffuse and, possibly, of reflected energy. In this case, a P&O (Perturbe and Observe) approach could be adopted. The measured values of solar power during the roof displacement from rest position to the predicted one can be utilized to identify a spatial model of solar power, so that to determine the optimal position of the roof taking into account all real world effects. In order that these measures are significant, an optimal PV panel control at each position should be performed by suitable Maximum Power Point Tracker (MPPT) techniques (Femia et al., 2008; Adinolfi et al., 2008). In addition, suitable algorithms could be used to process the images taken by a webcam, to detect the sun position and the actual sky conditions, in terms of cloudness and presence of shadows. In such way, it would be possible to avoid unnecessary roof movements, resulting in energy losses, when the actual sky conditions do not make the orientation convenient.

8. ECONOMIC FEASIBILITY

To assess the economic feasibility of a moving solar roof on a car, the payback time has been estimated as a function of the vehicle average generation efficiency of mechanical energy from fuel. In next graphs the payback of fixed (horizontal) and moving (ideal) roofs are compared, for two different latitudes (Los Angeles 33.9 and Minneapolis 44.9), using the insulation data provided by the database PVWatts (www.nrel.gov/rredc/pvwatts). It has been assumed PV panel efficiency η=18%, a battery charging/discharging efficiency of 0.9, PV area of 2 m^2 and fuel costs of 0.8 and 1.45 €/l, representative of USA and Italy; the roof cost has been computed by the following relationship:

$$C=C1+C2*A+C3 \quad (15)$$

where C1 (50 €) is a fixed cost for roof structure, C2 (300 €/m^2) is the unit cost of PV panels and C3 (200 €) is the cost for the orienting mechanism. The energy consumed for handling the solar roof has been neglected.

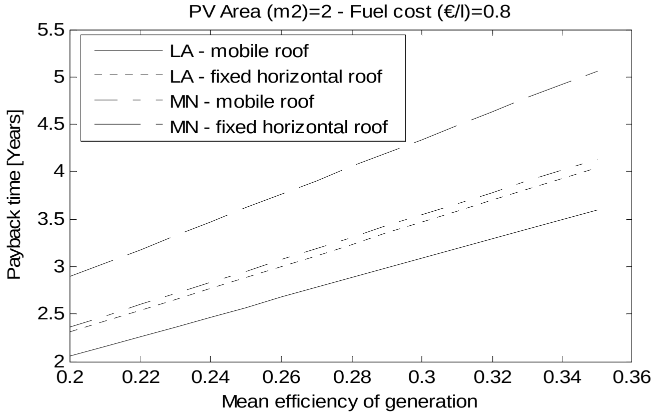

Fig. 16 Payback time for a fuel cost 0.8 €/l

It can be observed that the mobile roof exhibits better payback with respect to the fixed one, particularly at higher latitudes. As expected, the payback increases with latitude and when the fuel cost decreases. Very interesting payback values are achieved when fuel cost is higher, as in Italy now, but acceptable values are obtained also when fuel cost is lower, as in USA. Of course, the results depend on the assumption made on roof cost. It is timely to remark that the real payback could be higher than the values presented here, due to non ideal orienting capabilities of a real solar roof, to fuel consumption increase due to aerodynamic losses and to additional weight.

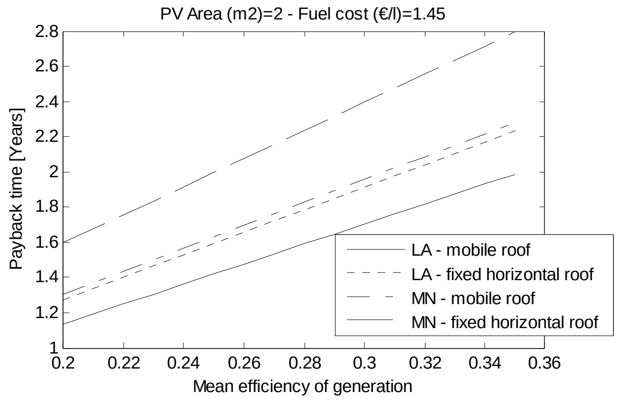

Fig. 17 Payback time for a fuel cost 1.45 €/l

9. CONCLUSIONS

The adoption of a moving solar roof can substantially enhance the energy recovered during parking phases, for a solar electric or hybrid vehicle. Moreover, this system can result particularly useful at high latitudes, where an horizontal panel would be strongly penalized by low sun height. The adoption of a moving roof can therefore extend the potential market of solar assisted vehicles. The kinematic model presented has allowed to optimize roof geometry and shape. The best orienting properties are reached with shapes approaching a circular one, and with the minimum distance between globular joints. The optimal solution has to be determined by an integrated analysis of both roof and vehicle shape.

The structure of a control system for real-time solar tracking in feed-forward and feedback mode has been also described. Economic feasibility has been also considered, with encouraging results. Further studies are in course to develop a real scale prototype of solar roof, to develop the model based control, and to evaluate the feasibility of such solution on vehicle.

REFERENCES

Adinolfi G., Arsie I., Di Martino R., Giustiniani A., Petrone G., Rizzo G., Sorrentino M. (2008) “A Prototype of Hybrid Solar Vehicle: Simulations and On-Board Measurements”, Proc. AVEC 2008, Oct.6-9, 2008, Kobe (Japan) 917-922 Soc.of Automotive Engineers of Japan - ISBN: 978-4-904056-21-9.

Arsie I., Di Martino R., Rizzo G., Sorrentino M. (2008, II) Energy Management for a Hybrid Solar Vehicle with Series Structure, *Proc. of 17th IFAC World Congress*, Seoul (Korea), July 6-11, 2008

Arsie I., Rizzo G., Sorrentino M. (2007) Optimal Design and Dynamic Simulation of a Hybrid Solar Vehicle, *SAE TRANSACTIONS - JOURNAL OF ENGINES* 115-3: 805-811

Arsie I., Rizzo G., Sorrentino M. (2008, I) A Model for the Optimal Design of a Hybrid Solar Vehicle *Review of Automotive Engineering*. Society of Automotive Engineers of Japan (JSAE) 29: 3. 439-447

Coraggio G. (2008), Progettazione di un tetto solare mobile per un veicolo ibrido solare. Master thesis, University of Salerno, (in Italian).

Femia N., Lisi G., Petrone G., Spagnuolo G., Vitelli M. (2008), “Distributed Maximum Power Point Tracking of Photovoltaic Arrays. Novel Approach and System Analysis” IEEE Transactions on Industrial Electronics Vol. 55, No. 7, July 2008, pp. 2610 - 2621.

Letendre S., Perez R., Herig C. (2003), Vehicle Integrated PV: A Clean and Secure Fuel for Hybrid Electric Vehicles, *Proc. of the American Solar Energy Society Solar 2003 Conference*, June 21-23, 2003, Austin,TX.

Pisanti C. (2008), Sviluppo di un modello matematico di un tetto solare mobile per un veicolo ibrido solare. Master thesis, University of Salerno, (in Italian).

Quaschning V. (2003), "Technology fundamentals - The sun as an energy resource". Renewable Energy World 6 (5): 90–93.

Rizzo G. (2010), “Automotive Applications of Solar Energy”, IFAC AAC 2010, Munich, July 11-14, 2010,

Statistics for Road Transport, UK Government, www.statistics.gov.uk/CCI/nscl.asp?ID=8100

Tsai L. W. (1999), Robot Analysis: the mechanics of serial and parallel manipulators, John Wiley & Sons, Inc., USA.

Appendix. THE KINEMATIC MODEL

In the following, the kinematic model of moving solar roof is presented. The geometry is defined by next figure, that represents the projection of the retractable roof on the horizontal plane. The variables are defined in the nomenclature. The coordinates of rectilinear cams can be computed through the following equations:

$$\begin{bmatrix} x_{s1} \\ x_{s2} \\ x_{s3} \\ y_{s1} \\ y_{s2} \\ y_{s3} \end{bmatrix} = \begin{bmatrix} x_{o1} \\ x_{o2} \\ x_{o3} \\ y_{o1} \\ y_{o2} \\ y_{o3} \end{bmatrix} + \begin{bmatrix} cos(30) & 0 & 0 \\ 0 & -cos(30) & 0 \\ 0 & 0 & 0 \\ sin(30) & 0 & 0 \\ 0 & sin(30) & 0 \\ 0 & 0 & -1 \end{bmatrix} \begin{bmatrix} s1 \\ s2 \\ s3 \end{bmatrix} \quad (A.1)$$

while the coordinates of globular joints can be computed as:

$$\begin{bmatrix} x_{b1} \\ x_{b2} \\ x_{b3} \\ y_{b1} \\ y_{b2} \\ y_{b3} \\ z_{b1} \\ z_{b2} \\ z_{b3} \end{bmatrix} = \begin{bmatrix} x_{s1} \\ x_{s2} \\ x_{s3} \\ y_{s1} \\ y_{s2} \\ y_{s3} \\ 0 \\ 0 \\ 0 \end{bmatrix} + \begin{bmatrix} c1\,cos\,30 & 0 & 0 \\ 0 & -c2\,cos\,30 & 0 \\ 0 & 0 & 0 \\ c1\,sin\,30 & 0 & 0 \\ 0 & c2\,sin\,30 & 0 \\ 0 & 0 & -c3 \\ s1 & 0 & 0 \\ 0 & s2 & 0 \\ 0 & 0 & s3 \end{bmatrix} \begin{bmatrix} r1 \\ r2 \\ r3 \end{bmatrix} \quad (A.2)$$

In this equation, it is $c1=\cos(\alpha 1)$, $c2=\cos(\alpha 2)$, $c3=\cos(\alpha 3)$, $s1=\sin(\alpha 1)$, $s2=\sin(\alpha 2)$, $s3=\sin(\alpha 3)$. The center of mass position and the computed length of legs are:

$$\bar{C} = \frac{\overline{B1} + \overline{B2} + \overline{B3}}{3} \quad (A.3)$$

$$l_c(i,j) = \sqrt{\left(x_{bi} - x_{bj}\right)^2 + (y_{bi} - y_{bj})^2 + (z_{bi} - z_{bj})^2} \quad (A.4)$$

The normal to the plane of the mobile roof is identified by three angles obtained in this way:

$$A = [x_{b1} y_{b1} 1; x_{b2} y_{b2} 1; x_{b3} y_{b3} 1] \quad (A.5)$$

$$B = [z_{b1}; z_{b2}; z_{b3}] \quad (A.6)$$

$$k = A/B \quad (A.7)$$

$$\beta_{x,y,z} = arctg\big(k(1,2,3)\big) \quad (A.8)$$

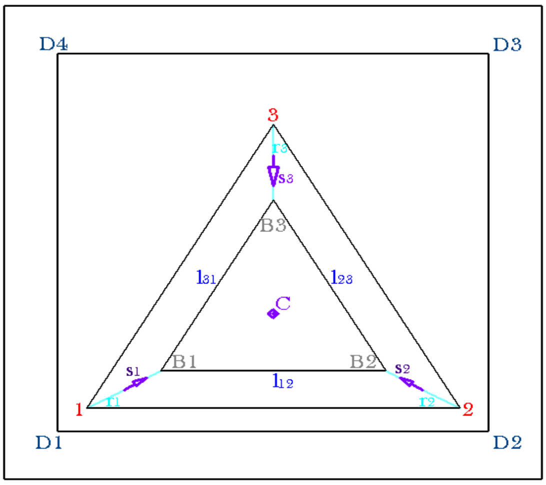

Fig. 18 Scheme of solar roof geometry

NOMENCLATURE

α	deg	Angle between rectilinear cam and leg
β	deg	Angle between solar roof and vehicle roof
δ	deg	Solar declination
φ	deg	Latitude
ϑ_s	deg	Sun height
h	deg	Hour angle
i	deg	Angle of incidence of solar ray
l	m	Distance between globular joints
l_c	m	Calculated l
N	/	Year day index
r	m	Leg length
s	m	Sliding of rectilinear cam
x,y,z	m	Coordinates of solar roof
x_0,y_0,z_0	m	Coordinates of rectilinear cams at rest
x_b,y_b,z_b	m	Coordinates of globular joints
x_c,y_c,z_c	m	Coordinates of center of solar roof
x_s,y_s,z_s	m	Coordinates of rectilinear cams
ϕ	deg	Azimuth whit respect to South
Pedices		
s	Sun	
v	Vehicle	
D1,D2,D3	Zenith of the roof	